

Make VLM Recognize Visual Hallucination on Cartoon Character Image with Pose Information

Bumsoo Kim^{1*}, Wonseop Shin^{1*}, Kyuchul Lee^{2‡}, Yonghoon Jung¹, Sanghyun Seo^{1†}

¹Chung-Ang University, ²Coupang

{^{1*}bumsookim, ^{1*}wonseop218, ¹dydgns2017, ^{1†}sanghyun}@cau.ac.kr, ^{2‡}kylee287@coupang.com

Abstract

Leveraging large-scale Text-to-Image (TTI) models have become a common technique for generating exemplar or training dataset in the fields of image synthesis, video editing, 3D reconstruction. However, semantic structural visual hallucinations involving perceptually severe defects remain a concern, especially in the domain of non-photorealistic rendering (NPR) such as cartoons and pixelization-style character. To detect these hallucinations in NPR, We propose a novel semantic structural hallucination detection system using Vision-Language Model (VLM). Our approach is to leverage the emerging capability of large language model, in-context learning which denotes that VLM has seen some examples by user for specific downstream task, here hallucination detection. Based on in-context learning, we introduce pose-aware in-context visual learning (PA-ICVL) which improve the overall performance of VLM by further inputting visual data beyond prompts, RGB images and pose information. By incorporating pose guidance, we enable VLMs to make more accurate decisions. Experimental results demonstrate significant improvements in identifying visual hallucinations compared to baseline methods relying solely on RGB images. Within selected two VLMs, GPT-4v, Gemini pro vision, our proposed PA-ICVL improves the hallucination detection with 50% to 78%, 57% to 80%, respectively. This research advances a capability of TTI models toward real-world applications by mitigating visual hallucinations via in-context visual learning, expanding their potential in non-photorealistic domains. In addition, it showcase how users can boost the downstream-specialized capability of open VLM by harnessing additional conditions. We collect synthetic cartoon-hallucination dataset with TTI models, this dataset and final tuned VLM will be publicly available. The dataset and demo VLMs are provided in the corresponding page: <https://gh-bumsookim.github.io/Cartoon-Hallucinations-Detection/>.

*Equal contributor

‡Project leader

†Corresponding author

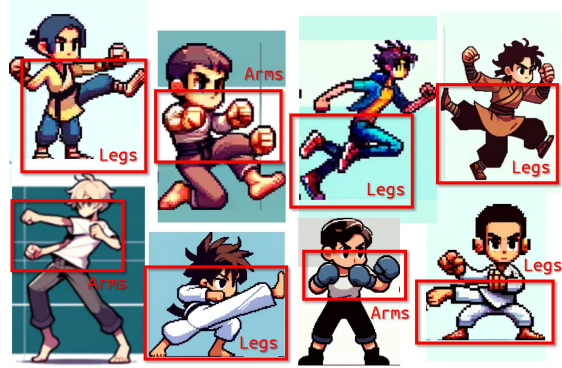


Figure 1. Examples of *semantic structural hallucination* in cartoon/pixel rendering images generated by TTI models. These hallucination hinder the TTI model to be extended toward applications, additionally requiring that users embark on burdensome process of eliminating hallucination sample in manual. More samples can be found in Appendices C.

1. Introduction

Leveraging machine-generated images based on large Text-to-Image (TTI) models [29, 30, 32, 34] has become a prominent, efficient technique in the field of image synthesis [41], video generation [7], 3D reconstruction [37, 43]. Recently, beyond TTI generation, complex multi-modal approaches combining Visual Language Models (VLMs) [1, 2, 23, 33, 44] upon Large Language Models (LLMs) [36, 47] are being utilized together with TTI to obtain more compelling, imaginative and plausible images. This is achieved by using reference images [45] or human-level image captioning [15] with multi-turn prompting under the advantages of in-context visual learning [38, 46].

However, TTI and VLMs [22] often suffer from the visual hallucination problem, similar to the hallucination issue in language models under LLMs [16, 40]. In image and video formats, a phenomenon, we denote it as *semantic structural hallucination*, occurs when images appear clear at first glance but show major inaccuracies upon closer examination as shown in Fig. 1. This means that even though the



Figure 2. Structural gap between real hallucination samples from normal prompt and fake hallucination samples from deliberately designed hallucination prompt. We highlight that generated fake hallucination samples (b) (intentionally generated by *hallucination prompt*) is not enough to imitate real one, limiting to generate large data sample.

images seem correct initially, they actually contain errors that become obvious when you look more closely. These inaccuracies compromise the models’ reliability and trustworthiness, posing challenges for network training and the broader adoption of large-scale generative models. Recent work, Vision language models are blind [31], explored the seven BlindTest, a basic visual tasks, and identified that VLM has frequently failed to understand the visual structure with textual prompts. It demonstrated that VLM has a still room to be enhanced toward specific task, remaining several frontier to be explored, even for basic visual mission.

Recent progress in the field of in-context visual learning has shown promising results in addressing various computer vision tasks. It is realized upon the advantages of in-context learning [8] which is a prominent capability of model to specialize the existing VLMs or LLMs to desired new tasks rapidly within a context without separated training or tuning stage. The seminal work by Wang et al. [38] introduced the concept of concatenating images to enable the application of a single model to multiple tasks. Zhang et al. [46] further extended this approach by proposing a prompt retrieval framework to automatically select the most relevant examples for a given query, leading to improved performance. Additionally, integrating multiple example samples into a single grid image has been shown to enhance performance as the number of examples increases [46]. Meanwhile, FAITHSCORE [17] proposed to evaluate various hallucination types with VLMs.

Nevertheless, these approaches have primarily focused on photorealistic images, and their effectiveness in non-photorealistic rendering (NPR) domains, such as cartoon characters, remains unexplored. Cartoon and pixel-style images, which represent non-photorealistic rendering [4,

19, 20, 39, 41], pose unique challenges due to their distinctive appearance and the difficulty in collecting large-scale datasets [18, 39, 41]. Consequently, generating cartoon-style characters via TTI models often results in frequent *semantic structural hallucinations*, such as characters with three legs or one arm, as shown in Fig. ?? . To address this problem, a dedicated refinement or post-processing step is necessary. However, to the best of our knowledge, no research has been conducted to specifically tackle this issue in cartoon-style images.

To bridge this gap, we present a novel visual hallucination detection system based on few-shot pose-aware in-context visual learning (PA-ICVL) in NPR domains. Our approach takes inspiration from recent progress in the area of in-context visual learning [38, 46]. However, we extend these methods to address the unique challenges posed by cartoon character images by incorporating numerical pose information alongside the visual data, necessitating a novel adaptation of the existing techniques. In PA-ICVL, we do not perform additional parameter training or tuning on the given input-output pairs. Instead, we leverage a capability of in-context visual learning that gradually provides the model with both visual and pose information. This enables our model to effectively utilize the in-context learning paradigm for the specific new task of visual hallucination detection in non-photorealistic domains, allowing VLMs to make more accurate decisions in identifying visual hallucinations. Our contributions include:

1. To the best of our knowledge, we first proposed visual hallucination detection system on non-photorealistic rendering domain, especially for machine-generated character images by text-to-image model, collecting a new public cartoon-hallucination dataset.
2. Within a capability of in-context visual learning on VLMs, we improve the detection accuracy with few-shot paired samples including RGB image, hallucination label and human-readable prompt.
3. To further enhance the detection performance, posture information is leveraged which demonstrate significant accuracy improvement by fine-tuning the pose estimator with pixel-cartoon domain images.

2. Challenges in Detecting Visual Hallucinations

Before our proposal, we conducted pre-analysis and trials to detect visual hallucinations without the use of VLMs with in-context visual learning. Initially, we sought to employ image classification by generating a dataset with labels, yet we were confronted with a data imbalance issue due to the unpredictable and uneven generation of hallucination

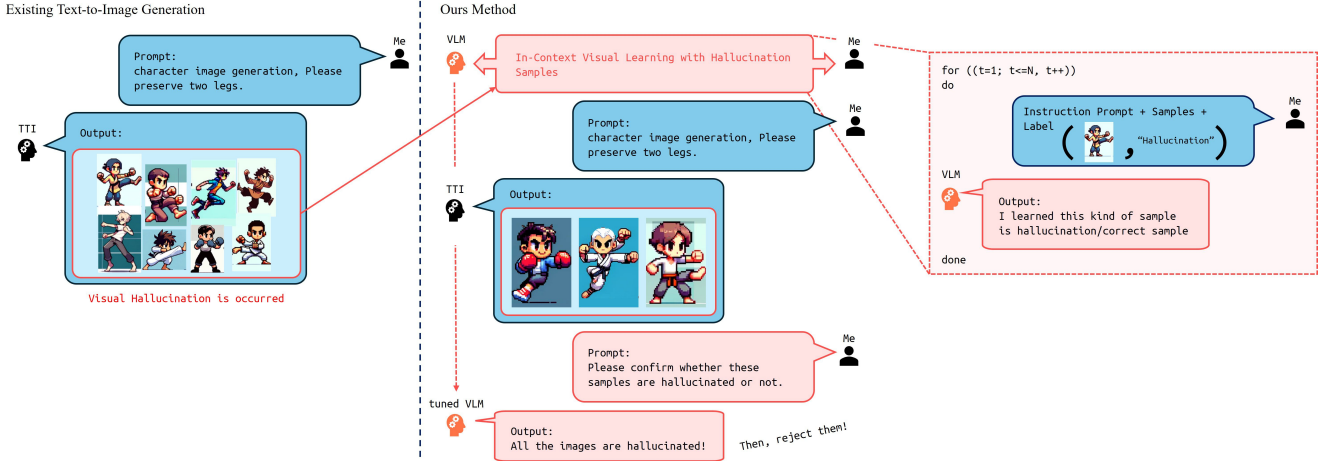


Figure 3. Schematic comparison to leverage machine-generated images between using existing TTI process and using our proposed method with in-context learned VLM for hallucination verification. Our goal is to detect hallucinations in images generated from TTI using VLM.

samples from the TTI process. In an effort to mitigate this challenge, we experimented with the deliberate generation of hallucination samples. However, this approach led us to face a gap in appearance between real and fabricated hallucinations. Through these endeavors, we concluded that amassing a large dataset for hallucination samples is not only limited but also a non-trivial task. This realization prompted us to explore the potential of learning from a few samples for the detection of hallucinations. In later sections, we provide some insights and detailed limitations through pre-analysis and trials to detect hallucination without VLMs.

2.1. Class Imbalance Problem

Our first approach was to adopt image classification to detect it by generating hallucination dataset with label. To do that, we wanted to gather correct (*i.e.*, non-hallucination) and hallucination samples through multiple TTI process. However we encountered data imbalance problem due to the fact that hallucination sample is unpredictably and unevenly generated with few samples from all the output according to textual prompts. Empirically, we faced about 10 hallucination samples per 100 images, but it is highly unpredictable according to input prompt and settings. From these observations, we concluded that gathering hallucination samples with iterative TTI is burdensome and inefficient.

2.2. Imitating Hallucination

To address aforementioned class imbalance issue, we wanted to generate synthetic dataset for hallucination samples deliberately such as [5, 28] with *hallucination prompt*, but faced appearance gap problem between real and fake hallucination as depicted in Fig. 2. We found that deliberately generated samples through our hallucination prompt

has exaggerated structure (Fig. 2b.) much far ways than real hallucination (Fig. 2a). Thus, we concluded that deliberately synthesizing large dataset for hallucination samples is also non-trivial and limited, and it makes us use few-samples for hallucination detection.

3. Methodology

Our goal is to recognize *semantic structural hallucination* in generated image by TTI using a capability of in-context learning on VLMs, as illustrated in Fig. 3. To do that, we first collect hallucination-aware cartoon character dataset (Sec. 3.1). Then, we demonstrate how posture information can be used in PA-ICVL (Sec. 3.2). Finally, it is explained how VLM make the decision in hallucination detection step (sec. 3.3)

3.1. Hallucination-aware Cartoon Dataset

To conduct PA-ICVL within a VLM, we delicately collect the cartoon hallucination dataset. Concretely, given input prompt \mathbf{P}_{input}^1 , cartoon character image $\mathbf{X}_{unknown}$ is generated as $\mathbf{X}_{unknown} = f(\mathbf{P}_{input})$ where $f(\cdot)$ is a TTI model. Through manual human annotation, label \mathbf{T}_* and description \mathbf{P}_{desc} are allocated while revealing $\mathbf{X}_{unknown}$ to \mathbf{X}_{known} . By repeating this step, hallucination-aware dataset \mathcal{D}^H is validated as $\mathcal{D}^H = ([\mathbf{X}_{known}^1, \mathbf{T}_*, \mathbf{P}_{desc}^1], \dots, [\mathbf{X}_{known}^N, \mathbf{T}_*, \mathbf{P}_{desc}^N])$ where N is the number of samples. In each sample, \mathbf{P}_{desc}^t is t -th description prompt which includes the explanation about why this sample is hallucinated/correct, \mathbf{T}_* is the t -th label where $*$ is known or unknown, and is obtained as $\mathbf{T}_h^t = \text{"This is hallucinated one"}$ or $\mathbf{T}_c^t =$

¹We provide used prompt in Appendices H.

Algorithm 1 PA-ICVL

Input: Hallucination dataset $\mathcal{D}^H = ([\mathbf{X}_{\text{known}}^1, \mathbf{M}_{\text{known}}^1, \mathbf{T}_*^1, \mathbf{P}_{\text{desc}}^1], \dots, [\mathbf{X}_{\text{known}}^N, \mathbf{M}_{\text{known}}^N, \mathbf{T}_*^N, \mathbf{P}_{\text{desc}}^N])$, system prompt \mathbf{P}_{sys} , a general-purpose VLM $g(\cdot)$.

Output: learned VLM $\hat{g}(\cdot)$

```

1:  $t \leftarrow 1$ 
2: // Initialize VLM
3:  $\hat{g}_0(\cdot) \leftarrow g(\mathbf{P}_{\text{sys}})$ 
4: while  $t \neq N+1$  do
5:    $\mathbf{X}_{\text{known}}^t, \mathbf{M}_{\text{known}}^t, \mathbf{T}_*^t, \mathbf{P}_{\text{desc}}^t \leftarrow \mathcal{D}^H$ 
6:   // PA-ICVL
7:    $\hat{\mathbf{T}}_*^t \leftarrow \hat{g}_{t-1}(\mathbf{X}_{\text{known}}^t, \mathbf{M}_{\text{known}}^t, \mathbf{P}_{\text{desc}}^t)$ 
8:   if  $\hat{\mathbf{T}}_*^t == \mathbf{T}_*^t$  then
9:      $\hat{g}_t(\cdot) \leftarrow \hat{g}_{t-1}(\cdot)$ 
10:     $t \leftarrow t+1$ 
11:   end if
12: end while
13: return  $\hat{g}_N(\cdot)$ 

```

"This is correct one" for a hallucination and a correct sample, respectively.

3.2. Pose-Aware In-Context Visual Learning

In the hallucination sample (Fig. 1), we found that visual hallucination samples from the cartoon domain include body structure issues such as arms, legs or heads. Based on these observations, we decide to leverage pose information to further improve the detection performance of VLM.

Given pre-trained pose estimator $\mathcal{E}_\theta(\cdot)$ which has weights θ obtained by training from the cartoon-domain, pose map \mathbf{M} is extracted as $\mathbf{M}_* = \mathcal{E}_\theta(\mathbf{X}_*)$ where \mathbf{M}_* has the same resolution as the input image \mathbf{X}_* and contains the pose joint information as the channel-axis. Thus, final each input of PA-ICVL for VLM is set as $[\mathbf{X}_{\text{known}}^t, \mathbf{M}_{\text{known}}^t, \mathbf{T}_*^t, \mathbf{P}_{\text{desc}}^t]$ where $\mathbf{M}_{\text{known}}^t$ is t -th pose map from $\mathbf{X}_{\text{known}}^t$. Each pose map \mathbf{M} contains pose information about the human structure, and the data structure changes depending on the experiments described in Sec. 4.2. Details about pose estimator $\mathcal{E}_\theta(\cdot)$ is described in Appendices G. After PA-ICVL outlined in the Alg. 1, a hallucination-aware VLM $\hat{g}_N(\cdot)$ is obtained which is ready to detect visual hallucinations in inference step (Sec. 3.3).

3.3. Visual Hallucination Detection

Till now, we explained how VLM learn visual hallucination based on in-context learning without updating parameters. Here, we describe how the hallucination-aware VLM can be utilized when faced with hallucination-unknown samples. Let's say newly generated image $\mathbf{X}_{\text{unknown}}$ is generated by user using TTI model, the pose estimator first $\mathcal{E}_\theta(\cdot)$ extracts a pose map as $\mathbf{M}_{\text{unknown}} = \mathcal{E}_\theta(\mathbf{X}_{\text{unknown}})$. Then,

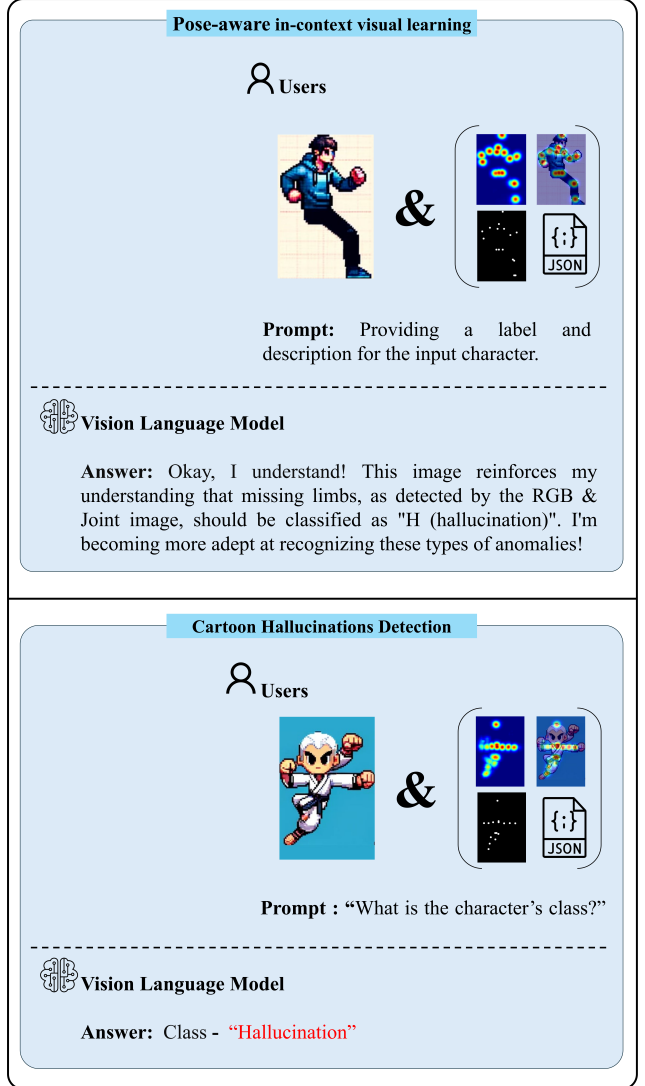


Figure 4. Example of PA-ICVL step (top) and detection step (bottom).

hallucination-aware VLM $\hat{g}_N(\cdot)$ predict hallucination label $\hat{\mathbf{T}}_p$ as $\hat{\mathbf{T}}_p = \hat{g}_N(\mathbf{X}_{\text{unknown}}, \mathbf{M}_{\text{unknown}})$. Finally, hallucination-unknown one $\mathbf{X}_{\text{unknown}}$ is determined as :

$$\mathbf{X}_{\text{unknown}} = \begin{cases} \hat{\mathbf{X}}_{\text{known}, c} & \text{if } \hat{\mathbf{T}}_p = \mathbf{T}_c \\ \hat{\mathbf{X}}_{\text{known}, h} & \text{if } \hat{\mathbf{T}}_p = \mathbf{T}_h \end{cases} \quad (1)$$

Example of PA-ICVL with detection is shown in Fig. 4. After detecting all the samples in new hallucination-unknown dataset, this dataset $\{\mathbf{X}_{\text{unknown}}\}$ is validated as hallucination-known dataset $\{\hat{\mathbf{X}}_{\text{known}, c}\}$, i.e., non-hallucinated samples with different the number of samples. Overall pipeline for hallucination detection process is illustrated in Fig. 5.

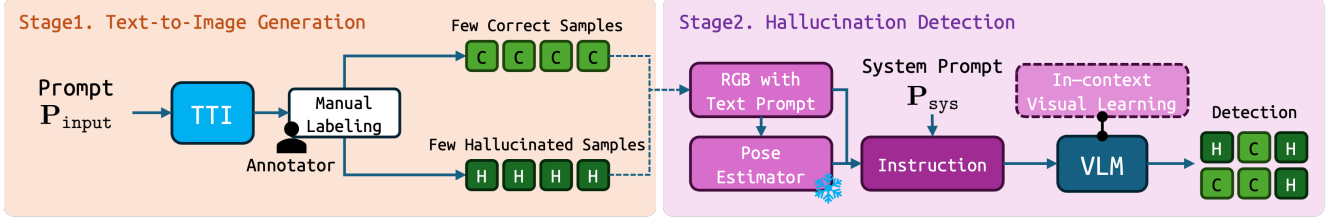


Figure 5. Pipeline of cartoon-hallucination dataset collection (Stage 1) and hallucination detection (Stage 2).

4. Experiments

4.1. Experimental Settings

For character appearance, we limit the style as cartoon and pixel using prompt which include an expression about human-like structure with five-head-figure². For TTI model, we adopt DALL-E3³ [6]. This is because we found that other TTI models (SDv1.5 [34], PixArt- α [11, 12] and so on) cannot generate consistent appearance (see Appendices D for TTI comparison). Final TTI image \mathbf{X} and input size of pose estimation has 384 by 256. For pose information, we used MPII [3] format for joint labeling which is represented as 16 joint feature as raw pose map \mathbf{M} . Details on fine-tuning pose estimator are included in Appendices G.2. For VLMs, GPT-4.0 Vision [1], Gemini 1.5 Pro [33] are selected.

4.2. Quantitative Evaluation with Ablation

VLM learned our state using the 5 correct and 5 hallucination train samples (total $N = 10$ images for PA-ICVL)⁴ and detect the test samples using 60 images for each class (total 120 images for evaluation) in our dataset. Dataset samples are shown in Fig. 7. To quantitatively evaluate the performance, we calculated the number of correct predictions relative to the total number of test samples for each class. This metric provides a clear indication of the learned VLM’s ability to accurately detect visual hallucinations in machine-generated pixel character images.

To verify the effectiveness of our method, we conduct ablation study as shown in Tab. 1. Model A is system prompt only VLMs. Model B is system prompt with the definition about hallucination. Model C is visual in-context learning. Multiple models D are our methods, PA-ICVL with various pose map format as shown in Fig. 6. \mathbf{M}_{gau} is Gaussian heatmap extracted from final convolution layer of pose estimator, \mathbf{M}_{over} is an overlay image using \mathbf{X} and \mathbf{M}_{gau} , \mathbf{M}_{xy} is final output of the pose estimator, which has the maximum value of each channel of \mathbf{M}_{gau} as the (x, y)

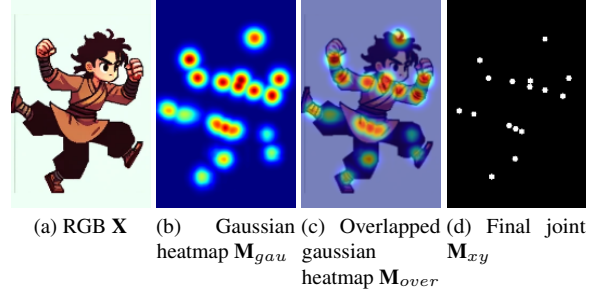


Figure 6. Example of input data about VLM for ablation study.

coordinates.

Model	Task Name	Inputs for VLM
A	System Prompt	.
B	A + Hallucination Define.	.
C	B + In-Context Learning	\mathbf{X}
D	Pose Guidance	
D-1	C + Gaussian Heatmap	$\mathbf{X}, \mathbf{M}_{gau}$
D-2	C + Only Overlapped Heatmap	\mathbf{M}_{over}
D-3	C + Overlapped Heatmap	$\mathbf{X}, \mathbf{M}_{over}$
D-4	C + Joint (image)	$\mathbf{X}, \mathbf{M}_{xy}$
D-5 [†]	C + Joint (text)	$\mathbf{X}, \text{text}(\mathbf{M}_{xy})$

Table 1. Ablation list. [†] denotes our final model

From ablation results in Fig. 8, our quantitative results demonstrate that model A seems to detect inputs randomly with about 50% accuracy, while model B shows a better score than model A, but still performs poorly. In contrast, model C, which learned from our hallucination cases, exhibits significantly better detection performance in both VLMs. Building upon this foundation, pose-aware models D-1, D-2, D-3 and D-4 demonstrate improved performance thanks to the additional pose input within GPT-4.0 Vision. In contrast, these additional inputs \mathbf{M}_{gau} , \mathbf{M}_{over} and \mathbf{M}_{xy} seems like to disturb the interpretation process in the case of Gemini 1.5 Pro with rather lower score. We conjecture this tendency is derived from that visual encoder equipped in GPT-4.0 Vision

²Note that descriptions of non-human-like cartoon characters are in the Appendices F.

³Note that we found meaningful tendency between ChatGPT platform and pure DALL-E3 API. We invite reader to Appendices E for details.

⁴Note that the results for the number of N are in the Appendices A.

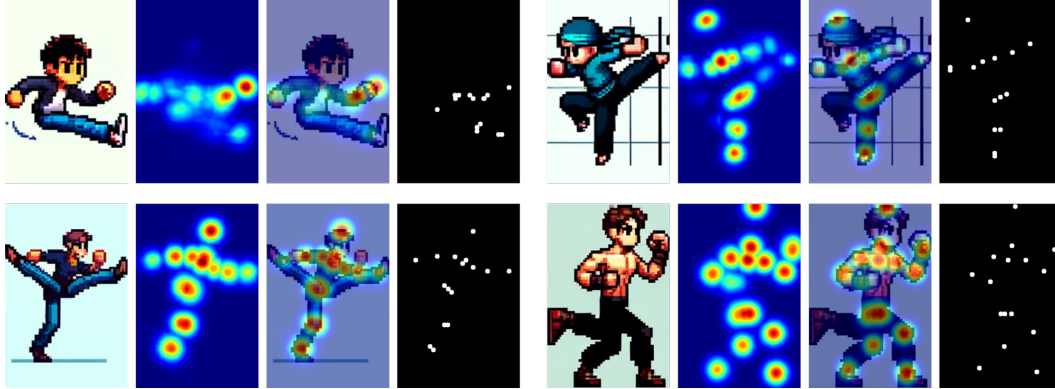


Figure 7. Samples of our cartoon-hallucination dataset.

Method	Subject	Approach	Cost per infer
Ours	Computer	PA-ICVL	663 tokens & 3 sec
Manual	Human	heuristic	None & 45 sec

Table 2. Cost approximation in detecting hallucination. Note that the cost of the proposed method is based on the average number of tokens (input tokens + output tokens) and the time it takes to inference, while the cost of the manual approach include \mathbf{P}_{desc} .

has a more prominent capability to understand various RGB image excluding general appearance than those of Gemini 1.5 Pro. Beyond using the image modality for pose, the language modality-based pose-aware model **D-5** achieves the best score in both VLMs. We argue that textual joint data can provide more precise posture information, enabling the VLM to effectively compare the input RGB image with the pose data to identify hallucinations.

4.3. Cost Prediction of Hallucination Detection

In terms of cost-effective feasibility, we compared the estimated detection costs of our proposed method against manual visual labeling. There is no existing method to detect cartoon hallucination, and training hallucination models with large samples is challenging, as discussed in Sec. 2. Therefore, we only compared our method to manual labeling based on human perception.

In our PA-ICVL method, the average input to infer one character consists of about 513 tokens, assuming an RGB image and keypoint JSON file combined with a prompt (e.g., ‘What is this character’s class?’). The images used in our experiments were 384x256 pixels, with each image using 255 tokens and the corresponding keypoint JSON file using 258 tokens. The total input tokens for inferring 120 characters amounted to 62.7K. VLM outputs an average of 140 tokens per character for classification and description, totaling about 17K tokens for all characters. Inference for

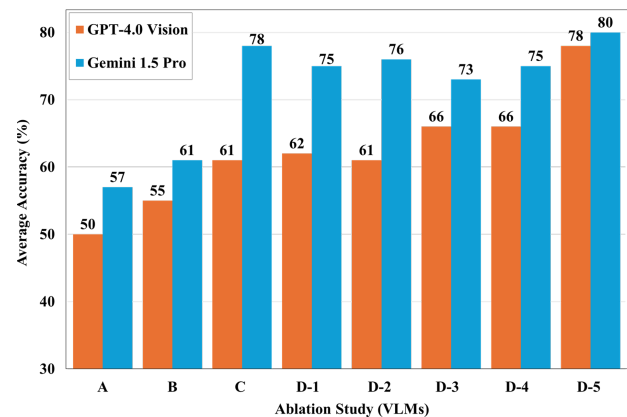


Figure 8. Quantitative evaluation with ablation study about *semantic structural hallucination* detection.

the entire dataset took approximately 10 minutes, excluding the 1-2 hour fine-tuning step of the pose estimator on an NVIDIA RTX 3090. After training, inference for our whole dataset using the pose estimation model took just 25 seconds.

For the manual detection process, two participants classified the same characters. They were asked to identify the images, classify them into separate folders, and add captions \mathbf{P}_{desc} explaining why the sample was hallucinated/corrected. Each inference step for this took an average of 45 seconds, and the entire process lasted approximately 1 hour and 30 minutes. No hallucination samples were provided, and participants were only given a definition of hallucination based on Model B. Overall comparison between two approaches is shown in Tab. 2.

5. Discussion

This section, we discuss about applications and extendability of our proposed method, hoping that it can serve as some insights or inspirations for multi-modal communities

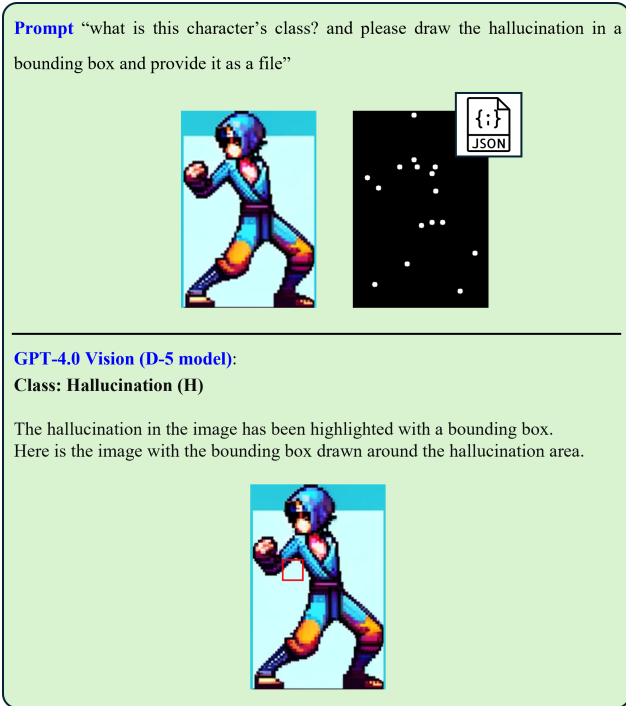


Figure 9. Visualization of hallucination region localization of VLM. **Red** bounding box denotes what VLM extract as dominant region to detect *semantic structural hallucination*.

and other researchers.

Our domain, cartoon style character, has extremely wide appearance. What is more, some cases include ambiguous appearance even in human cognition. Therefore, our learned VLM can not detect all the images of wide-range cartoon style. Meanwhile, in the perspective of model capabilities, it is known that TTI models and VLMs tend to generate output sensitively with word position-bias, verbosity-bias, self-enhancement-bias [48]. Due to that, it is noteworthy that output or results can be showed as quite different tendency according to the inputs. Through above mentioned things, we would like to mention that there are some limitations to leverage our scheme toward more generalized task directly. Following description include our attempts and faced limitations with some specific application cases.

5.1. Limitation: Hallucination-Region Localization

We wanted to exploit hallucination region toward several applications such as regional restoration by feeding finding region as desired masking map (e.g., in-painting [24]). To do this, we let the tuned VLM extract and visualize the structural hallucination region as rectangular bounding box.

In toy experiments as shown in Fig. 9, we observed that VLM failed to extract hallucination elements in given images. To improve this, it can be considered that in-context visual learning is conducted with an annotated bounding box information of hallucination elements. We note that Gemini

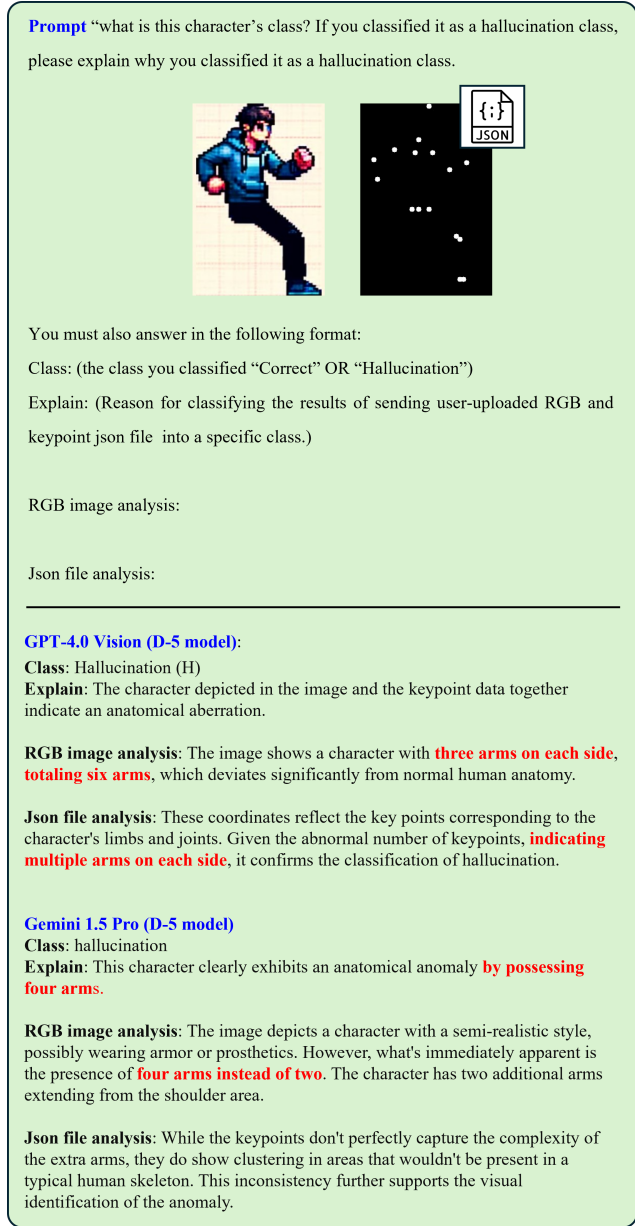


Figure 10. Explanations about the reason of hallucination. We denotes wrong explanation as **Red-bold** font.

1.5 Pro is excluded in this test since they have not yet that function for drawing bounding box.

5.2. Limitation: Explainability

As a continuation of Sec. 5.1, we also would like to explore the explainability of VLMs about hallucination detection. By doing that, we expect to understand how VLMs reason the hallucination within given samples beyond the classification. Here, we instructed the VLMs to explain the detailed reason about their decision as a textual prompt. As

shown in Fig. 10, it is observed that description capability of each VLM is insufficient to explain the hallucination elements. Therefore, as a result, we mention that explaining the reason via VLMs can not always ensure the correct answers.

5.3. Future Works

In this paper, the range of visual hallucination appearance was limited as character structure with five-head-figure. However, more natural scene (*e.g.*, video or 3D) for real-world contain wide structure. For instance, some images has not contain full-body. For future work, we intent to detect partial and detailed hallucination like fingers and would like to realize restoration about hallucination region based on region localization as discussed in Sec. 5.1. Moreover, generalizability for realistic images will be included in advanced version of our works.

6. Conclusion

Our research has introduced a novel visual hallucination detection system for cartoon character images generated by large-scale TTI models. To address this issue, inspired by recent progress in in-context visual learning, we leveraged PA-ICVL, integrating RGB images with pose information from a fine-tuned pose estimator. This method extends existing in-context visual learning strategies by adding numerical pose data to visual inputs, utilizing a distinctive repetitive information injection approach. By iteratively feeding visual and pose data into the model within a contextual history, our system leverages the advantages of in-context learning with no additional training. Moreover, we collected a cartoon-hallucination dataset with corresponding pose maps which will be publicly available. As a result, VLMs have become more precise in identifying visual hallucinations. Our experiments have demonstrated that our approach significantly improves upon baseline methods, notably enhancing TTI models by mitigating visual hallucinations and broadening their applicability, particularly in scenarios where visual accuracy is paramount. Specifically, through testing under various pose information conditions, we found that incorporating language modal-based joint information proved to be the most effective strategy. In addition, our experiments showed that external condition can reinforce the visual understanding capabilities of VLM by improving task-specific performance, achieving 78%, 80% detection performance from 50%, 57% about GPT-4v, Gemini pro vision, respectively. These experimental results convey the significant insight where general VLM can be specialized to each domain by taking advantages of in-context visual learning with external information. Future work will aim to integrate additional modalities and adapt our approach to various non/photorealistic styles, enhancing TTI model applications. Our method, addressing cartoon image challenges, establishes new benchmarks in detecting visual hallucinations in such domains.

Acknowledgments

This research was supported by Culture, Sports and Tourism R&D Program through the Korea Creative Content Agency grant funded by Ministry of Culture, Sports and Tourism in 2024 (Project Name : Developing Professionals for R&D in Contents Production Based on Generative Ai and Cloud, Project Number : RS-2024-00352578, Contribution Rate: 50%) and Culture, Sports and Tourism R&D Program through the Korea Creative Content Agency (KOCCA) grant funded by the Ministry of Culture, Sports and Tourism (MCST) in 2023 (Project Name: Development of digital abusing detection and management technology for a safe Metaverse service, Project Number: RS-2023-00227686, Contribution Rate: 50%) and Artificial intelligence industrial convergence cluster development project funded by the Ministry of Science and ICT(MSIT, Korea) & Gwangju Metropolitan City.

References

- [1] Josh Achiam, Steven Adler, Sandhini Agarwal, Lama Ahmad, Ilge Akkaya, Florencia Leoni Aleman, Diogo Almeida, Janko Altenschmidt, Sam Altman, Shyamal Anadkat, et al. Gpt-4 technical report. *arXiv preprint arXiv:2303.08774*, 2023. 1, 5
- [2] Jean-Baptiste Alayrac, Jeff Donahue, Pauline Luc, Antoine Miech, Iain Barr, Yana Hasson, Karel Lenc, Arthur Mensch, Katherine Millican, Malcolm Reynolds, et al. Flamingo: a visual language model for few-shot learning. *Advances in Neural Information Processing Systems*, 35:23716–23736, 2022. 1
- [3] Mykhaylo Andriluka, Leonid Pishchulin, Peter Gehler, and Bernt Schiele. 2d human pose estimation: New benchmark and state of the art analysis. In *IEEE Conference on Computer Vision and Pattern Recognition (CVPR)*, June 2014. 5
- [4] Jihye Back, Seungkwon Kim, and Namhyuk Ahn. Webtoonme: A data-centric approach for full-body portrait stylization. In *SIGGRAPH Asia 2022 Technical Communications*, pages 1–4. ACM, 2022. 2
- [5] Haoran Bai, Di Kang, Haoxian Zhang, Jinshan Pan, and Linchao Bao. Ffhq-uv: Normalized facial uv-texture dataset for 3d face reconstruction. In *Proceedings of the IEEE/CVF Conference on Computer Vision and Pattern Recognition*, pages 362–371, 2023. 3
- [6] James Betker, Gabriel Goh, Li Jing, Tim Brooks, Jianfeng Wang, Linjie Li, Long Ouyang, Juntang Zhuang, Joyce Lee, Yufei Guo, et al. Improving image generation with better captions. *Computer Science*. <https://cdn.openai.com/papers/dall-e-3.pdf>, 2(3):8, 2023. 5, 11, 12
- [7] Andreas Blattmann, Tim Dockhorn, Sumith Kulal, Daniel Mendelevitch, Maciej Kilian, Dominik Lorenz, Yam Levi, Zion English, Vikram Voleti, Adam Letts, et al. Stable video diffusion: Scaling latent video diffusion models to large datasets. *arXiv preprint arXiv:2311.15127*, 2023. 1
- [8] Tom Brown, Benjamin Mann, Nick Ryder, Melanie Subbiah, Jared D Kaplan, Prafulla Dhariwal, Arvind Neelakantan, Pranav Shyam, Girish Sastry, Amanda Askell, et al. Language

- models are few-shot learners. *Advances in neural information processing systems*, 33:1877–1901, 2020. **2**
- [9] Sanghyun Byun, Bumsoo Kim, Wonseop Shin, Yonghoon Jung, and Sanghyun Seo. Transfer learning based parameterized 3d mesh deformation with 2d stylized cartoon character. *KSII Transactions on Internet & Information Systems*, 17(11), 2023. **13**
- [10] Z. Cao, G. Hidalgo Martinez, T. Simon, S. Wei, and Y. A. Sheikh. Openpose: Realtime multi-person 2d pose estimation using part affinity fields. *IEEE Transactions on Pattern Analysis and Machine Intelligence*, 2019. **13**
- [11] Junsong Chen, Yue Wu, Simian Luo, Enze Xie, Sayak Paul, Ping Luo, Hang Zhao, and Zhenguo Li. Pixart- δ : Fast and controllable image generation with latent consistency models, 2024. **5**
- [12] Junsong Chen, Jincheng Yu, Chongjian Ge, Lewei Yao, Enze Xie, Yue Wu, Zhongdao Wang, James Kwok, Ping Luo, Huchuan Lu, and Zhenguo Li. Pixart- α : Fast training of diffusion transformer for photorealistic text-to-image synthesis, 2023. **5, 11, 12**
- [13] Haodong Duan, Kwan-Yee Lin, Sheng Jin, Wentao Liu, Chen Qian, and Wanli Ouyang. Trb: a novel triplet representation for understanding 2d human body. In *Proceedings of the IEEE/CVF international conference on computer vision*, pages 9479–9488, 2019. **13**
- [14] Or Hirschorn and Shai Avidan. Pose anything: A graph-based approach for category-agnostic pose estimation. *arXiv preprint arXiv:2311.17891*, 2023. **13**
- [15] Xiaowei Hu, Zhe Gan, Jianfeng Wang, Zhengyuan Yang, Zicheng Liu, Yumao Lu, and Lijuan Wang. Scaling up vision-language pre-training for image captioning. In *Proceedings of the IEEE/CVF conference on computer vision and pattern recognition*, pages 17980–17989, 2022. **1**
- [16] Lei Huang, Weijiang Yu, Weitao Ma, Weihong Zhong, Zhangyin Feng, Haotian Wang, Qianglong Chen, Weihua Peng, Xiaocheng Feng, Bing Qin, et al. A survey on hallucination in large language models: Principles, taxonomy, challenges, and open questions. *arXiv preprint arXiv:2311.05232*, 2023. **1**
- [17] Liqiang Jing, Ruosen Li, Yunmo Chen, Mengzhao Jia, and Xinya Du. Faithscore: Evaluating hallucinations in large vision-language models. *arXiv preprint arXiv:2311.01477*, 2023. **2**
- [18] Bumsoo Kim, Sanghyun Byun, Yonghoon Jung, Wonseop Shin, Sareer UI Amin, and Sanghyun Seo. Minecraft-ify: Minecraft style image generation with text-guided image editing for in-game application. *arXiv preprint arXiv:2402.05448*, 2024. **2**
- [19] Bumsoo Kim, Abdul Muqet, Kyuchul Lee, and Sanghyun Seo. Toonaging: Face re-aging upon artistic portrait style transfer. *arXiv preprint arXiv:2402.02733*, 2024. **2**
- [20] Seungkwon Kim, Chaeheon Gwak, Dohyun Kim, Kwangho Lee, Jihye Back, Namhyuk Ahn, and Daesik Kim. Cross-domain style mixing for face cartoonization. *arXiv preprint arXiv:2205.12450*, 2022. **2**
- [21] Donghoon Lee, Jiseob Kim, Jisu Choi, Jongmin Kim, Minwoo Byeon, Woonhyuk Baek, and Saehoon Kim. Karlo-v1.0.alpha on coyo-100m and cc15m. <https://github.com/kakaobrain/karlo>, 2022. **11, 12**
- [22] Yifan Li, Yifan Du, Kun Zhou, Jinpeng Wang, Wayne Xin Zhao, and Ji-Rong Wen. Evaluating object hallucination in large vision-language models. *arXiv preprint arXiv:2305.10355*, 2023. **1**
- [23] Haotian Liu, Chunyuan Li, Qingyang Wu, and Yong Jae Lee. Visual instruction tuning. *Advances in neural information processing systems*, 36, 2024. **1**
- [24] Andreas Lugmayr, Martin Danelljan, Andres Romero, Fisher Yu, Radu Timofte, and Luc Van Gool. Repaint: Inpainting using denoising diffusion probabilistic models. In *Proceedings of the IEEE/CVF conference on computer vision and pattern recognition*, pages 11461–11471, 2022. **7**
- [25] Simian Luo, Yiqin Tan, Longbo Huang, Jian Li, and Hang Zhao. Latent consistency models: Synthesizing high-resolution images with few-step inference, 2023. **11, 12**
- [26] Simian Luo, Yiqin Tan, Suraj Patil, Daniel Gu, Patrick von Platen, Apolinário Passos, Longbo Huang, Jian Li, and Hang Zhao. Lcm-lora: A universal stable-diffusion acceleration module. *arXiv preprint arXiv:2311.05556*, 2023. **11**
- [27] MMPose Contributors. OpenMMLab Pose Estimation Toolbox and Benchmark. <https://github.com/open-mmlab/mmpose>, Aug. 2020. License: Apache-2.0. **13**
- [28] Abdul Muqet, Kyuchul Lee, Bumsoo Kim, Yohan Hong, Hyunrae Lee, Woonggon Kim, and KwangHee Lee. Video face re-aging: Toward temporally consistent face re-aging. *arXiv preprint arXiv:2311.11642*, 2023. **3**
- [29] Alex Nichol, Prafulla Dhariwal, Aditya Ramesh, Pranav Shyam, Pamela Mishkin, Bob McGrew, Ilya Sutskever, and Mark Chen. Glide: Towards photorealistic image generation and editing with text-guided diffusion models. *arXiv preprint arXiv:2112.10741*, 2021. **1**
- [30] Dustin Podell, Zion English, Kyle Lacey, Andreas Blattmann, Tim Dockhorn, Jonas Müller, Joe Penna, and Robin Rombach. Sdxl: Improving latent diffusion models for high-resolution image synthesis. *arXiv preprint arXiv:2307.01952*, 2023. **1, 11, 12**
- [31] Pooyan Rahmazadehgervi, Logan Bolton, Mohammad Reza Taesiri, and Anh Totti Nguyen. Vision language models are blind. *arXiv preprint arXiv:2407.06581*, 2024. **2**
- [32] Aditya Ramesh, Mikhail Pavlov, Gabriel Goh, Scott Gray, Chelsea Voss, Alec Radford, Mark Chen, and Ilya Sutskever. Zero-shot text-to-image generation. In *International Conference on Machine Learning*, pages 8821–8831. PMLR, 2021. **1**
- [33] Machel Reid, Nikolay Savinov, Denis Teplyashin, Dmitry Lepikhin, Timothy Lillicrap, Jean-baptiste Alayrac, Radu Soricut, Angeliki Lazaridou, Orhan Firat, Julian Schrittwieser, et al. Gemini 1.5: Unlocking multimodal understanding across millions of tokens of context. *arXiv preprint arXiv:2403.05530*, 2024. **1, 5**
- [34] Robin Rombach, Andreas Blattmann, Dominik Lorenz, Patrick Esser, and Björn Ommer. High-resolution image synthesis with latent diffusion models. In *Proceedings of the IEEE/CVF conference on computer vision and pattern recognition*, pages 10684–10695, 2022. **1, 5**

- [35] Ke Sun, Bin Xiao, Dong Liu, and Jingdong Wang. Deep high-resolution representation learning for human pose estimation. In *Proceedings of the IEEE/CVF conference on computer vision and pattern recognition*, pages 5693–5703, 2019. [13](#)
- [36] Hugo Touvron, Thibaut Lavril, Gautier Izacard, Xavier Martinet, Marie-Anne Lachaux, Timothée Lacroix, Baptiste Rozière, Naman Goyal, Eric Hambro, Faisal Azhar, et al. Llama: Open and efficient foundation language models. *arXiv preprint arXiv:2302.13971*, 2023. [1](#)
- [37] Vikram Voleti, Chun-Han Yao, Mark Boss, Adam Letts, David Pankratz, Dmitry Tochilkin, Christian Laforte, Robin Rombach, and Varun Jampani. Sv3d: Novel multi-view synthesis and 3d generation from a single image using latent video diffusion. *arXiv preprint arXiv:2403.12008*, 2024. [1](#)
- [38] Xinlong Wang, Wen Wang, Yue Cao, Chunhua Shen, and Tiejun Huang. Images speak in images: A generalist painter for in-context visual learning. In *Proceedings of the IEEE/CVF Conference on Computer Vision and Pattern Recognition*, pages 6830–6839, 2023. [1](#), [2](#)
- [39] Zongwei Wu, Liangyu Chai, Nanxuan Zhao, Bailin Deng, Yongtuo Liu, Qiang Wen, Junle Wang, and Shengfeng He. Make your own sprites: Aliasing-aware and cell-controllable pixelization. *ACM Transactions on Graphics (TOG)*, 41(6):1–16, 2022. [2](#)
- [40] Ziwei Xu, Sanjay Jain, and Mohan Kankanhalli. Hallucination is inevitable: An innate limitation of large language models. *arXiv preprint arXiv:2401.11817*, 2024. [1](#)
- [41] Shuai Yang, Liming Jiang, Ziwei Liu, and Chen Change Loy. Pastiche master: Exemplar-based high-resolution portrait style transfer. In *Proceedings of the IEEE/CVF Conference on Computer Vision and Pattern Recognition*, pages 7693–7702, 2022. [1](#), [2](#)
- [42] Yi Yang and Deva Ramanan. Articulated pose estimation with flexible mixtures-of-parts. In *CVPR 2011*, pages 1385–1392. IEEE, 2011. [13](#)
- [43] Chi Zhang, Yiwen Chen, Yijun Fu, Zhenglin Zhou, Gang Yu, Billzb Wang, Bin Fu, Tao Chen, Guosheng Lin, and Chunhua Shen. Styleavatar3d: Leveraging image-text diffusion models for high-fidelity 3d avatar generation. *arXiv preprint arXiv:2305.19012*, 2023. [1](#)
- [44] Jingyi Zhang, Jiaying Huang, Sheng Jin, and Shijian Lu. Vision-language models for vision tasks: A survey. *arXiv preprint arXiv:2304.00685*, 2023. [1](#)
- [45] Lvmin Zhang, Anyi Rao, and Maneesh Agrawala. Adding conditional control to text-to-image diffusion models. In *Proceedings of the IEEE/CVF International Conference on Computer Vision*, pages 3836–3847, 2023. [1](#)
- [46] Yuanhan Zhang, Kaiyang Zhou, and Ziwei Liu. What makes good examples for visual in-context learning? *Advances in Neural Information Processing Systems*, 36, 2024. [1](#), [2](#)
- [47] Wayne Xin Zhao, Kun Zhou, Junyi Li, Tianyi Tang, Xiaolei Wang, Yupeng Hou, Yingqian Min, Beichen Zhang, Junjie Zhang, Zican Dong, et al. A survey of large language models. *arXiv preprint arXiv:2303.18223*, 2023. [1](#)
- [48] Lianmin Zheng, Wei-Lin Chiang, Ying Sheng, Siyuan Zhuang, Zhanghao Wu, Yonghao Zhuang, Zi Lin, Zhuohan Li, Dacheng Li, Eric Xing, et al. Judging llm-as-a-judge with

mt-bench and chatbot arena. *Advances in Neural Information Processing Systems*, 36, 2024. [7](#)

A. Fewer Samples for PA-ICVL

We demonstrate how the number of samples N for PA-ICVL impacts on results. Including 5 samples for each class used in the main experiments, we gradually reduced the number of samples to 1 and 3. When we applied in-context learning, we saw that different values of N resulted in different detection results, which is shown in Tab. 3

Model (D-5)	$N = 1$	$N = 3$	$N = 5$
GPT-4 Vision	71%	73%	78%
Gemini 1.5 Pro	72%	73%	80%

Table 3. Results of final model according to the number of N .

B. Results on Image Transformation

Based on the appearance of our dataset, it can be inferred that VLM may focus on the leg or arm regions. Thus, detecting hallucination might be easy in our settings. To address this conjecture, we separately evaluate the hallucination detection performance of two VLMs by flipping and rotating images. The evaluation results for character images flipped horizontally relative to the base model (D5) did not differ significantly. When evaluated using character images rotated 0.5π , there was a significant difference in accuracy. The evaluation results are shown in Tab. 1. This gap could mean that the VLM does not recognise rotated character images correctly, as opposed to forward facing characters.

Model (D-5)	Base	Horizontal-Flip	0.5π Rotation
GPT-4 Vision	78%	76%	54%
Gemini 1.5 Pro	80%	77%	61%

Table 4. Results according to image transformation

C. Visual Hallucination in Cartoon Domain

Cartoon domain has unique appearance. The cases and level of visual hallucination are quite different from realistic domain. When we generate many cartoon image from TTI, we found that there are two classes about hallucination tendency as shown in Fig. 11: one is uncompleted whole-body having one arm, one leg or even no head as shown in Fig. 11a, other one is over-depiction of body components such as three arms, three legs as shown in Fig. 11b. These hallucination types led us utilize pose estimation for visual hallucination detection in cartoon image.



Figure 11. Hallucination classes in cartoon domain.

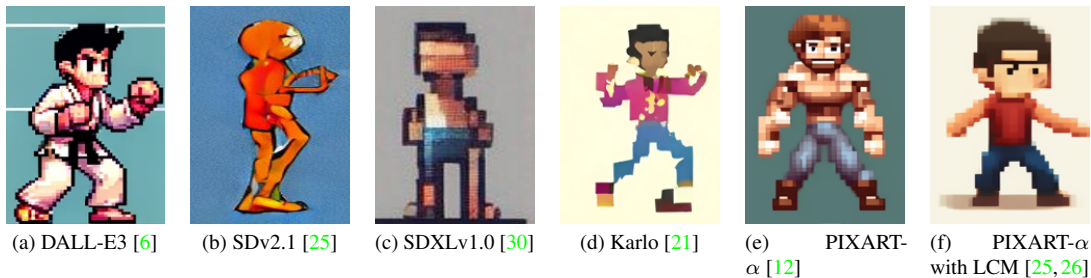


Figure 12. Comparison for cartoon rendering quality with SOTA TTI models

D. Cartoon Rendering Comparison with Various Large TTI Models

We evaluate TTI models which include DALL-E3 [6], SDv2.1⁵ [25], SDXLv1.0⁶ [30], Karlo⁷ [21], PIXART- α ⁸ [12], PIXART- α with LCM⁹. For comparison in terms of cartoon rendering quality, we used same input prompt for every TTI models. For Karlo, the input prompts we used were also converted to combinations of words because, in Karlo website, we found that user typically used word format rather than sentences.

As shown in Fig. 12, we found that all the models generate non-plausible appearance for cartoon-pixel character except DALL-E3. Due to that, we used DALL-E3 for our TTI model.

E. ChatGPT-4 Vision vs DALL-E3 API

We found that there are some gaps about appearance tendency between ChatGPT-4 Vision through ChatGPT site¹⁰ and pure DALL-E3 API¹¹. We conducted experiments by feeding the TTI prompts into both ChatGPT-4 Vision and the DALL-E3 API to generate images. Empirically, we observed that ChatGPT-4 Vision created images that were closer to our desired output with clean apparent structure compared to DALL-E3 API. We conjecture that this result is derived from ChatGPT’s capability to refine and analyze the provided prompt, which in turn elevates its comprehension of the prompt, leading to the production of superior images.

F. Non-Human-like Cartoon Character

We would like to extend the applicability of ours to non-human-like cartoon characters. To do so, we wanted to evaluate these samples by finding suitable input prompts for them. However, it was observed that the pose estimator was unable to extract accurate pose joints as shown in Fig. 13. Thus we cannot conduct evaluations with non-human-like character under the conclusion that pose guidance would not provide useful information to VLMs in PA-ICVL step.

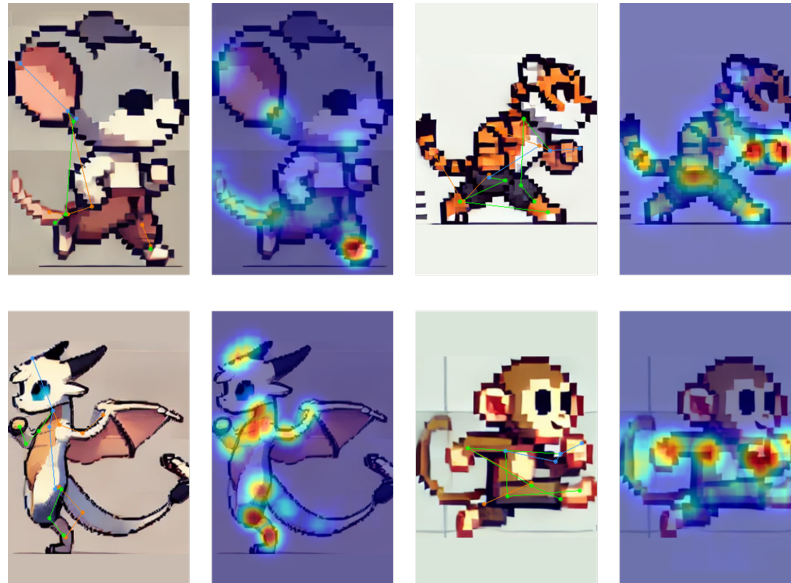


Figure 13. Failed pose estimation on non-human-like character.

⁵<https://huggingface.co/spaces/stabilityai/stable-diffusion>

⁶<https://huggingface.co/stabilityai/stable-diffusion-xl-base-1.0>

⁷<https://karlo.ai/>

⁸<https://huggingface.co/spaces/PixArt-alpha/PixArt-alpha>

⁹<https://huggingface.co/spaces/PixArt-alpha/PixArt-LCM>

¹⁰<https://openai.com/gpt-4>

¹¹<https://openai.com/dall-e-3>

G. Pose Estimator

Here, we provide some details for our pose estimator including fine-tuning scheme and comparison on other off-the-shelf pose estimators.

G.1. Comparison on Various Pose Estimators

To use visually precise pose joint about cartoon character to VLM, we used our fine-tuned pose estimator (see Appendices G.2 for details of fine-tuning). Here, we show the pose estimation performance with off-the-shelf pose estimators which include PoseAnything [14], OpenPose [10]. For PoseAnything, we used 1-Shot split-1 small model from official repository¹². For OpenPose, we used pose_iter_160000.caffemodel for MPII format from official repository¹³.



Figure 14. Comparison of pose estimation.

As shown in Fig. 14, we found that there is no one which can predict perceptually plausible joint. This is conjectured that cartoon domain distributed far away from pre-trained weights, leading requirement of fine-tuning with this domain.

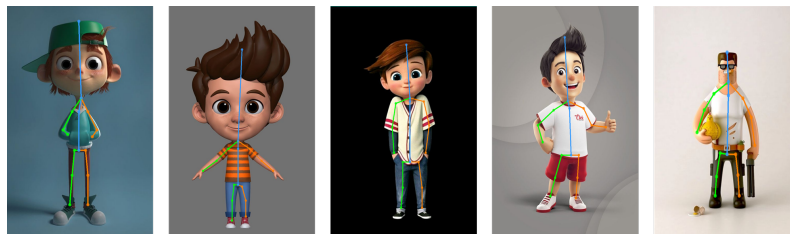


Figure 15. Example of training dataset for pose estimation fine-tuning.

G.2. Fine-tuning

We fine-tune the pose estimator based on HRNet-w48 [35] (Top-down approach) upon MMPose library [27] with collected 3D cartoon dataset as shown in Fig. 15. Our training scheme is based on [9]. For pose estimation settings, we used MPII-TRB [13] keypoint format (16 joint for whole-body) with inference image size as 384 by 256 using boundary padding. Including 2D illustration and rendered 2D images from 3D model shape, totalling 2400 images in animation, illustration and cartoon domains are used for fine-tuning for about 16K iterations with 32 batch size, achieving 0.8902 PCKh (Percentage of Correct Key-points head) [42] at threshold 0.5.

H. Used prompts

H.1. TTI Input prompt list

1. Please design a 2D motion frame pixel style character with a size of 256x384 pixels. Each action should be displayed on a separate row, with the first row being a {kicking, punching, jumping, running, walking .. etc} action (composed of 5 frames) and the second row being a {kicking, punching, jumping, running, walking .. etc} action (composed of 5 frames) that appears

¹²<https://github.com/orhir/PoseAnything>

¹³<https://github.com/CMU-Perceptual-Computing-Lab/openpose>

to be smoothly connected. The generated actions should not overlap, and the character's color should be simple. The entire sprite sheet should be 1792x1024 in size.

2. (Without detailed color & overlap prompt) Please design a 2D pixel style character with a size of 256x384 pixels. Each action should be displayed on a separate row, with the first row being a {kicking, punching, jumping, running, walking .. etc} action (composed of 5 frames) and the second row being a {kicking, punching, jumping, running, walking .. etc} action (composed of 5 frames) that appears to be smoothly connected. The entire sprite sheet should be 1792x1024 in size.

3. (Without pixel size prompt) Please design a 2D motion frame pixel style character. Each action should be displayed on a separate row, with the first row being a {kicking, punching, jumping, running, walking .. etc} action and the second row being a {kicking, punching, jumping, running, walking .. etc} action that appears to be smoothly connected. The generated actions should not overlap, and the character's color should be simple. The entire sprite sheet should be 1792x1024 in size.

H.2. Instruction prompt list

System Prompt & Hallucination Definition : You are a hallucination detector, and your mission is to detect if the image has hallucinations. Here I define hallucination as when a character is missing an arm, leg, or has an abnormal number of them (three legs, three arms .. etc). So you need to detect the hallucination I defined in the image and visually describe the hallucination. So as a sample of how to detect this well, we'll provide the following prompts with a hallucination image, a normal image {and joint image, joint file, heatmap image}.

1. **(Model C)** Using RGB image - Correct class : This character is performing a {kicking, punching, jumping, running, walking .. etc} motion with an image of a correct human body with two arms and two legs. This image of a correct human anatomy will be classified as C (correct class) in the future. Your task is to recognize images with correct human anatomy as C images.

2. **(Model C)** Using RGB image - Hallucination class : This character is performing a {kicking, punching, jumping, running, walking .. etc} motion with an abnormal character with {three legs, three arms, no head, no arms, no legs, only one arm, only one leg}. This image of abnormal human anatomy will be classified as H (hallucination class) in the future. Your task is to recognize images with abnormal human anatomy as H images.

3. **(Model D-1)** Using RGB & Gaussian heatmap image - Correct class : This image is a pose heatmap obtained from the pose estimator. This character is performing a {kicking, punching, jumping, running, walking .. etc} motion with an image of a correct human body with two arms and two legs. This image of a correct human anatomy will be classified as C (correct class) in the future. Your task is to recognize images with correct human anatomy as C images.

4. **(Model D-1)** Using RGB & Gaussian heatmap image - Hallucination class : This image is a pose heatmap obtained from the pose estimator. This character is performing a {kicking, punching, jumping, running, walking .. etc} with {three legs, three arms, no head, no arms, no legs, only one arm, only one leg}. This image of abnormal human anatomy will be classified as H (hallucination class) in the future. Your task is to recognize images with abnormal human anatomy as H images.

5. **(Model D-2)** Using Overlapped heatmap image - Correct class : This image is a pose heatmap obtained from the pose estimator. This character is performing a {kicking, punching, jumping, running, walking .. etc} motion with an image of a correct human body with two arms and two legs. This image of a correct human anatomy will be classified as C (correct class) in the future. Your task is to recognize images with correct human anatomy as C images.

6. **(Model D-2)** Using Overlapped heatmap image - Hallucination class : This image is a pose heatmap obtained from the pose estimator. This character is performing a {kicking, punching, jumping, running, walking .. etc} with {three legs, three arms, no head, no arms, no legs, only one arm, only one leg}. This image of abnormal human anatomy will be classified as H (hallucination class) in the future. Your task is to recognize images with abnormal human anatomy as H images.

7. **(Model D-3)** Using RGB & overlapped heatmap image - Correct class : The first image is an RGB image of the character and the second image is a heatmap of the character's pose using the pose estimator. This character is performing a {kicking, punching, jumping, running, walking .. etc} motion with an image of a normal human body with two arms and two legs. This image of a normal human anatomy will be classified as C (correct class) in the future. Your task is to recognize images with

normal human anatomy as C images.

8. **(Model D-3)** Using RGB & overlapped heatmap image - Hallucination class : The first image is an RGB image of the character and the second image is a heatmap of the character's pose using the pose estimator. This character is performing a {kicking, punching, jumping, running, walking .. etc} motion with {three legs, three arms, no head, no arms, no legs, only one arm, only one leg}. This image of abnormal human anatomy will be classified as H (hallucination class) in the future. Your task is to recognize images with abnormal human anatomy as H images.

9. **(Model D-4)** Using RGB image & Joint (image) - Correct class : The first image is an RGB image of the character and the second image is a keypoint of the character's pose using the pose estimator. This character is performing a {kicking, punching, jumping, running, walking .. etc} motion with an image of a correct human body with two arms and two legs. This image of a correct human anatomy will be classified as C (correct class) in the future. Your task is to recognize images with correct human anatomy as C images.

10. **(Model D-4)** Using RGB image & Joint (image) - Hallucination class : The first image is an RGB image of the character and the second image is a keypoint of the character's pose using the pose estimator. This character is performing a {kicking, punching, jumping, running, walking .. etc} motion with an abnormal character with {three legs, three arms, no head, no arms, no legs, only one arm, only one leg}. This image of abnormal human anatomy will be classified as H (hallucination class) in the future. Your task is to recognize images with abnormal human anatomy as H images.

11. **(Model D-5)** Using RGB image & Joint (text) - Correct class : The first image is an RGB image of the character and the second file is a keypoint of the character's pose using the pose estimator. This character is performing a {kicking, punching, jumping, running, walking .. etc} motion with an image of a correct human body with two arms and two legs. This image of a correct human anatomy will be classified as C (correct class) in the future. Your task is to recognize images with correct human anatomy as C images.

12. **(Model D-5)** Using RGB image & Joint (text) - Hallucination class : The first image is an RGB image of the character and the second file is a keypoint of the character's pose using the pose estimator. This character is performing a {kicking, punching, jumping, running, walking .. etc} motion with an abnormal character with {three legs, three arms, no head, no arms, no legs, only one arm, only one leg}. This image of abnormal human anatomy will be classified as H (hallucination class) in the future. Your task is to recognize images with abnormal human anatomy as H images.